

Local current distribution in a ferromagnetic tunnel junction measured using conducting atomic force microscopy

著者	安藤 康夫
journal or publication title	Journal of applied physics
volume	87
number	9
page range	5206-5208
year	2000
URL	http://hdl.handle.net/10097/35845

doi: 10.1063/1.373296

Local current distribution in a ferromagnetic tunnel junction measured using conducting atomic force microscopy

Y. Ando,^{a)} H. Kameda, H. Kubota, and T. Miyazaki

Applied Physics, Graduate School of Engineering, Tohoku University, Aoba-yama 08, Sendai 980-8579, Japan

The local electrical properties were measured simultaneously with the topography for a Ta(50 Å)/Fe₂₀Ni₈₀(50 Å)/IrMn(150 Å)/Co(50 Å)/Al(13 Å)-oxide junction. The electrical image showed the contrast with around a few nm lateral size and a strong correlation with the topographical image was not observed. In the local current–voltage characteristics, data within the bias voltage of ± 1.5 V were fitted well to Simmons's equation and we obtained the barrier height $\Phi = 1.9$ eV and the thickness $d = 12$ Å. On the other hand, data with the bias voltages higher than 3 V were fitted well to Fowler–Nordheim equation. The histogram of current density was calculated by taking into consideration a Gaussian distribution of the barrier thickness and the height. The distribution of the barrier height can explain the experimental result realistically. © 2000 American Institute of Physics. [S0021-8979(00)54308-4]

I. INTRODUCTION

Ferromagnetic tunnel junctions have been extensively studied since the discovery of a large magnetoresistance ratio (TMR) at room temperature.^{1,2} These junctions are potentially applicable in magnetoresistive reading heads, magnetic field sensors, and nonvolatile magnetoresistive random access memories (MRAMs).^{3,4} In order to make them usable as industrial products, the barrier thickness and height must be accurately controlled to avoid fluctuations in resistance. However, there are a few techniques available to characterize electrical properties on a nanometer scale.

A scanning probe microscope (SPM) system including an atomic force microscope (AFM) and a scanning tunneling microscope (STM) is one of the most powerful instruments for achieving the characterization of electrical properties on a nanometer scale.^{5–7} We have reported the results of the contact AFM measurement with simultaneous detecting currents through the tunnel barrier.⁸ This technique provides the information of the local barrier characteristics not being affected by the surface roughness.⁹

In this article, we report the electrical images of the insulator in a ferromagnetic tunnel junction with various applied voltages. In order to obtain the distribution of the barrier characteristics quantitatively, the images and the local current–voltage (I – V) properties are analyzed in terms of a simple calculation that takes into account the Fowler–Nordheim type tunneling.¹⁰

II. EXPERIMENTAL PROCEDURE

A Ta(50 Å)/Fe₂₀Ni₈₀(50 Å)/IrMn(150 Å)/Co(50 Å)/Al(13 Å)-oxide junction was prepared on a thermally oxidized Si substrate by magnetron sputtering using an inductively coupled plasma (ICP).¹¹ The base pressure was below 5×10^{-6} Pa and the sputtering was carried out in an atmosphere of 0.08 Pa Ar. Oxidation of Al was performed by an

ICP oxidation method using an Ar+O₂ gas with a total pressure of 1 Pa. The applied power was 20 W and the oxidation time was 210 s. The details of these fabrication and oxidation methods were described in a previous article.^{8,11} Measurement of the local current distribution was carried out using a commercial AFM system. The triangular cantilever was made of silicon nitride and both sides were coated with about 40-nm-thick Au. The tip was scanned on the insulator surface while maintaining the atomic force constant by feedback, namely, the topographical image was provided by an ordinary contact-mode AFM. Simultaneously, a bias voltage between the substrate and the tip was applied and the current was mapped, resulting in an electrical image. We varied the bias voltage and the contact force between the sample and the tip. The sample was transferred from the fabrication chamber to the AFM system within a few minutes after breaking the vacuum, and all the measurements were performed under a pressure of less than 1×10^{-4} Pa. Because gas molecules adsorbed on the surface of a sample can result in changing tunneling currents, we carefully checked the influence of breaking the vacuum by changing the exposing time or annealing the sample below 200 °C, and concluded that a few minutes breaking of the vacuum was no influence on the electrical images.

III. RESULTS AND DISCUSSION

Figure 1 shows the topographical and electrical images measured simultaneously. The scanning area is 200×200 nm² and the bias voltage was 5 V. The topography is typical of the surface on Al oxide and the average roughness was 0.2 nm which is very smooth. In the electrical image, the bright areas indicate a high tunneling current, and there are the contrast of currents place to place. In order to confirm the correlation between the topography and the currents, the cross-sectional profiles of the height (broken lines) and current (solid lines) along the lines (a) and (b) in Fig. 1 are obtained and shown in Fig. 2. The average lateral size of the topographically high region is around 20 nm, while that of

^{a)}Electronic mail: ando@mlab.apph.tohoku.ac.jp

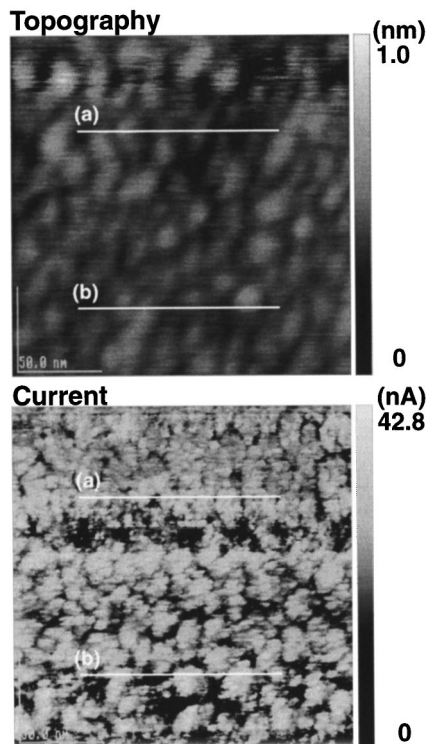


FIG. 1. The topographical and electrical images measured simultaneously. The bias voltage is 5 V and the scanning area is $200 \times 200 \text{ nm}^2$.

the electrically high region is only a few nm. And also, note that no strong correlation between the electrical and topographical images is observed. This result suggests that the current distributions are influenced very little by the roughness of the surfaces. They might say that when the bottom electrode consists of grains with narrow trenches between them, one will still detect local variations of the current if the perfect oxide barrier is present. However, this idea could not give any consistent explanation of the wide valley of the current profile observed along line (b). The cross-sectional image by transmission electron microscopy (TEM) separately measured¹² showed very smooth surface of the bottom electrode and its grain size corresponded to the lateral size of the topography. Therefore, the AFM tip can follow adequately the surface contours and the current image provides the local variations of the oxide barrier.

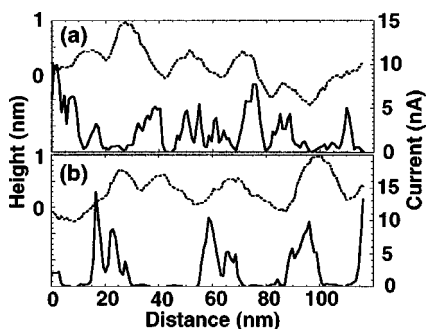


FIG. 2. The cross-sectional profiles of the height (broken lines) and current (solid lines) along the lines (a) and (b) in Fig. 1.

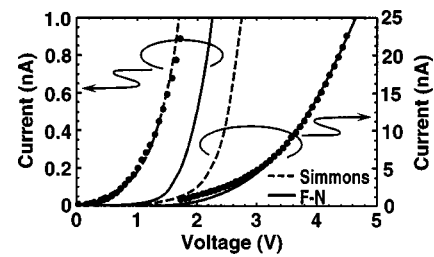


FIG. 3. The typical local $I-V$ characteristic indicated by closed circles. The broken and solid lines show the fitting results using Simmons' and Fowler-Nordheim equation, respectively.

The barrier height and its thickness are used to be estimated by measuring the $I-V$ curve. Figure 3 shows the example of the local $I-V$ curve indicated by closed circles. The current axis for the data of low bias voltages is enlarged. Simmons' equation is used generally to obtain the barrier height and thickness of the tunnel junction.¹³ Using the data within $\pm 1.5 \text{ V}$ and assuming an effective contact area of 100 nm^2 , we obtained the values of the barrier height $\Phi = 1.9 \text{ eV}$ and the thickness $d = 12 \text{ \AA}$. The broken line shows the fitting result. It fits to the data well at voltage lower than 1.5 V , while it increases drastically apart from the experimental result over the bias voltage of 2 V . Because Simmons' equation is effective only for low bias voltages, Fowler-Nordheim (F-N) equation should be used for the fitting to the data with a bias voltage much larger than Φ , where the current is due to tunneling of electrons through the triangular barrier into the oxide conduction band. The current-voltage relation will be expressed by

$$I = A_{\text{eff}} \frac{e^3 m_0}{8 \pi h m_{\text{eff}}} \frac{1}{t(E)^2} \frac{\beta^2 V^2}{\Phi d^2} \times \exp\left(-\frac{8 \pi \sqrt{2 m_{\text{eff}}}}{3 h e} \nu(E) \frac{d \Phi^{3/2}}{\beta V}\right), \quad (1)$$

where A_{eff} is the effective emission area at the injecting electrode, h is Planck's constant, e is a charge of electron and $m_{\text{eff}}/m_0 = 0.5$ is the effective mass of the electron in the conduction band of the insulator.⁷ Image charge lowering is taken into account by functions $\nu(E) = 0.93$ and $t(E) = 1$. The field enhancement factor β arises from the nonplanar geometry of the tip. Since we could not know the exact shape of the tip, we assumed that $\beta = 1$ and treated A_{eff} as a fitting parameter in following analysis. The fluctuation of A_{eff} was checked carefully and was little during at least one frame scanning. The solid line in Fig. 3 shows the fitting result using $\Phi = 1.9 \text{ eV}$, $d = 12.6 \text{ \AA}$, and $A_{\text{eff}} = 1.2 \times 10^{-20}$. The fitting is pretty good at a voltage higher than 3 V , namely, the increase of the currents at higher voltages can be explained by the F-N-type tunneling model. We measured $I-V$ curves also at several points and obtained the deviation of $\Phi = \pm 0.3 \text{ eV}$ and that of $d = \pm 0.5 \text{ \AA}$. However, these are the results on some limited sites, the $I-V$ measurement is not suitable to obtain the distribution of the tunneling barrier parameters quantitatively.

Figure 4 shows the current histogram statistically calculated from the electrical image indicated by closed circles.

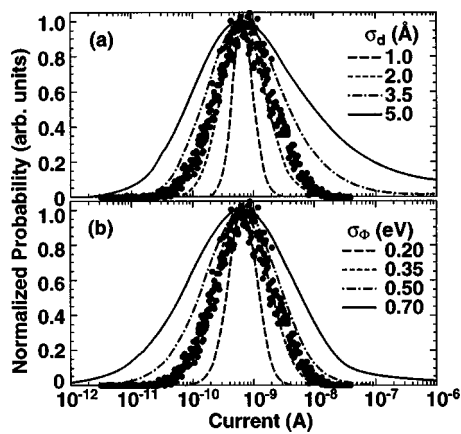


FIG. 4. The current histograms statistically obtained from the electrical images indicated by closed circles. The calculated probability of current density fitted for the experimental result are also shown in two cases. (a) The barrier thickness was assumed to distribute around the average value d_{ave} of 12 Å and the barrier height Φ was fixed at 1.9 eV. (b) The barrier height was assumed to distribute around the average value Φ_{ave} of 1.9 eV and the barrier thickness d was fixed at 12 Å.

The counts are normalized at the maximum value. Because it exhibits a large asymmetric shape and a long tail at high currents, it is shown in the figure by a logarithmic scale. The width of this histogram is considered to be local variations in the tunneling barrier height or thickness. We calculate the current distribution using a simple model and compare with the experimental results. The fluctuations of barrier height or barrier thickness are assumed to obey a Gaussian distribution. The tunnel currents can be calculated using Eq. (1) with these fluctuations of the barrier parameters. The results of the calculation are also shown in the figure. Figures 4(a) and 4(b) show the cases that the barrier height Φ is fixed at 1.9 eV and the barrier thickness d is fixed at 12 Å, respectively. In the (a) case, the average value of the barrier thickness d_{ave} is 12 Å and the deviation σ_d is varied between 1.0 and 5.0 Å. The probability of current density is strongly affected by σ_d ; remarkably, the half width increase with increasing σ_d . The experimental data seems to fit for the calculation with σ_d between 2.0 and 3.5 Å. On the other hand in the (b) case, the average value of the barrier height Φ_{ave} is 1.9 eV, and the deviation σ_Φ is varied between 0.2 and 0.7 eV. This calculation with σ_Φ of about 0.35 eV traces well the experimental result. Actually, both effects of (a) and (b) probably are mixed and could not be separated exactly. However, the σ_d of 3.5 Å seems to be too large to be expected by our separate TEM results.¹² Consequently, the contrast of the current im-

age is plausible to be the distribution of the barrier heights due to a lack of oxygen on an atomic level in comparison with the Al₂O₃ composition. Oxygen will enter a metallic Al layer through the grain boundaries at an early stage and diffuse inside the grains. The variations in the concentration of oxygen are considered to be generated in the process. Optimizing the fabrication condition of Al oxide may effectively decrease the σ_Φ .

IV. SUMMARY

We investigated the local electrical properties measured on a Ta/Fe₂₀Ni₈₀/IrMn/Co/Al-oxide junction using a conducting AFM. The local I - V characteristic at higher bias voltages was fitted well to the equation of F-N-type tunneling. Based on the simple model using F-N equation, it was plausible that the contrast of the current image indicated the distribution of the barrier heights. It will provide a guide to an accurately controlled ferromagnetic tunnel junction that maintains a high MR ratio even with a low tunnel resistance.

ACKNOWLEDGMENTS

This research was supported by Sumitomo Foundation, the Storage Research Consortium (SRC), Regional Consortium Project (NEDO), and Grant-in-Aids for Scientific Research (Priority Areas Nos. 09236101 and 11355001) from the Ministry of Education, Science, Sports, and Culture of Japan.

- ¹T. Miyazaki and N. Tezuka, *J. Magn. Magn. Mater.* **139**, L231 (1995).
- ²J. S. Moodera, L. R. Kinder, T. M. Wong, and R. Meservey, *Phys. Rev. Lett.* **74**, 3273 (1995).
- ³T. Miyazaki, N. Tezuka, S. Kumagai, Y. Ando, H. Kubota, J. Murai, T. Watabe, and M. Yokota, *J. Phys. D: Appl. Phys.* **31**, 630 (1998).
- ⁴S. S. P. Parkin, K. P. Roche, M. G. Samant, P. M. Rice, R. B. Beyers, R. E. Scheuerlein, E. J. O'Sullivan, S. L. Brown, J. Bucchigano, D. W. Abraham, Yu Lu M. Rooks, P. L. Trouilloud, R. A. Wanner, and W. J. Gallagher, *J. Appl. Phys.* **85**, 5828 (1999).
- ⁵R. Wiesendanger, M. Bode, R. Dombrowski, M. Getzlaff, M. Morgenstern, and C. Wittneven, *Jpn. J. Appl. Phys., Part 1* **37**, 3769 (1998).
- ⁶H. Tomiye, T. Yao, H. Kawami, and T. Hayase, *Appl. Phys. Lett.* **69**, 4050 (1986).
- ⁷A. Olbrich, B. Ebersberger, and C. Boit, *Appl. Phys. Lett.* **73**, 3114 (1998).
- ⁸Y. Ando, H. Kameda, H. Kubota, and T. Miyazaki, *Jpn. J. Appl. Phys., Part 2* **38**, L737 (1999).
- ⁹V. Da Costa, F. Bardou, C. Béal, Y. Henry, J. P. Bucher, and K. Ounadjela, *J. Appl. Phys.* **83**, 6703 (1998).
- ¹⁰M. Lenzlinger and E. H. Snow, *J. Appl. Phys.* **40**, 278 (1969).
- ¹¹J. Sugawara, E. Nakashio, S. Kumagai, J. Honda, Y. Ikeda, and T. Miyazaki, *J. Magn. Soc. Jpn.* **23**, 1281 (1999).
- ¹²T. Daibou, N. Tezuka, H. Kubota, Y. Ando, M. Hayashi, T. Miyazaki, C. Kim, and O. Song, *J. Magn. Soc. Jpn.* **24** (in press).
- ¹³N. Tezuka, Y. Ando, T. Miyazaki, H. G. Tompkins, S. Tehrani, and H. Goronkin, *J. Magn. Soc. Jpn.* **21**, 493 (1997).